

CHARMLESS B DECAYS INTO THREE CHARGED TRACK FINAL STATES

A. GARMASH

Budker Institute of Nuclear Physics, Novosibirsk, 630090, Russia

and

KEK, High Energy Accelerator Research Organization, Oho 1-1, Tsukuba, Ibaraki, Japan

E-mail: garmash@bmail.kek.jp

For the Belle Collaboration

Using a data sample of 10.5 fb^{-1} collected by the Belle detector, three-body charmless decays $B^+ \rightarrow K^+ h^+ h^-$ have been studied. The following branching fractions have been obtained: $\mathcal{B}(B^+ \rightarrow K^+ \pi^- \pi^+) = (64.8 \pm 10.0 \pm 7.0) \times 10^{-6}$ and $\mathcal{B}(B^+ \rightarrow K^+ K^- K^+) = (36.5 \pm 6.1 \pm 5.5) \times 10^{-6}$. The upper limits for other combinations of charged kaons and pions have been placed. Analysis of the intermediate two-body states gives evidence for production of scalar resonances in charmless B decays.

1 Introduction

Until recently charmless B decays were mainly studied via their two-body decay modes because of the large combinatorial background in multibody channels. In this work we attempt to study $B^+ \rightarrow K^+ h^+ h^-$ decays (h stands for a charged pion or kaon) without any assumption about the intermediate hadronic resonances. Reference to the charge conjugate states is implicit throughout this paper unless explicitly stated otherwise.

Analysis is based on the data set collected by the Belle detector¹ at KEKB², the asymmetric B -factory at KEK. It consists of 10.5 fb^{-1} taken at the $\Upsilon(4S)$ resonance and 0.6 fb^{-1} taken below the $B\bar{B}$ production threshold for continuum studies.

2 Event selection

Charged tracks are required to satisfy a set of track quality cuts based on the average hit residual and the impact parameters in both the $r - \phi$ and $r - z$ planes. We require that the transverse track momenta be greater than $100 \text{ MeV}/c$ to reduce low momentum combinatorial background.

The candidate events are identified by using the beam-constrained mass $M_{bc} = \sqrt{(\sqrt{s}/2)^2 - P_B^{*2}}$ and the calculated energy difference $\Delta E = E_B^* - \sqrt{s}/2$ where E_B^* and P_B^* are the energy and 3-momentum of the B candidate in the $\Upsilon(4S)$ rest frame. We define the B signal region as: $5.271 < M_{bc} < 5.289 \text{ GeV}/c^2$; $|\Delta E| < 40 \text{ MeV}$.

The most important issues of this analysis are efficient kaon identification over the whole momentum region and the suppression of the large combinatorial background which is dominated by $q\bar{q}$ continuum production.

Since two B mesons produced from the $\Upsilon(4S)$ decay are nearly at rest in the CMS frame, the angles of the decay products of two B 's are uncorrelated and the event looks spherical. In contrast, hadrons from continuum $q\bar{q}$

events tend to exhibit a two-jet structure.

We calculate the angle, θ_{Thr} , between the thrust axis of the B candidate and that of the rest of the event. The distribution of $|\cos(\theta_{Thr})|$ is strongly peaked near 1.0 for $q\bar{q}$ events while it is nearly flat for $B\bar{B}$ events. We require $|\cos(\theta_{Thr})| < 0.80$ for all modes under consideration.

We also form a Fisher discriminant³ with the momentum scalar sum of charged particles and photons in nine cones of increasing polar angle around the thrust axis of the B candidate and the angle of the thrust axis of the candidate with respect to the beam axis. We combine the Fisher discriminant and $\cos(\theta_B)$, where θ_B is the angle between the B candidate momentum and the beam axis, in a single variable by taking a product of the corresponding probability density functions and impose a cut on the likelihood ratio.

Separation of kaons and pions is accomplished by combining the responses of the ACC and the TOF with dE/dx measurements in the CDC. The combined response of the three systems provides high quality K/π separation in the laboratory momentum range up to $3.5 \text{ GeV}/c$. At large momenta only the ACC and dE/dx are used since here TOF provides no significant separation of kaons and pions.

3 Analysis

In this analysis at least one charged track was required to be positively identified as a kaon. Then we considered all possible combinations of charged kaons and pions. The analysis of $K^+ \pi^+ \pi^-$ and $K^+ K^+ K^-$ final states is described in detail in two following subsections. The results on the study of other combinations are summarized in Table 2.

3.1 $B^+ \rightarrow K^+ \pi^+ \pi^-$

To study this final state we require one track to be positively identified as a kaon and two tracks consis-

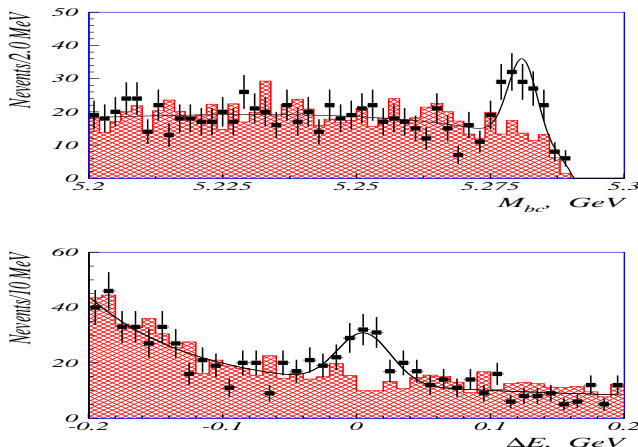


Figure 1: The M_{bc} (top) and ΔE (bottom) distributions for selected $B^+ \rightarrow K^+\pi^+\pi^-$ candidates. Points are data and histograms are Monte Carlo expectation for background. Curves are fit to the data.

tent with the pion hypothesis. The contributions from $B^+ \rightarrow \bar{D}^0\pi^+$ where $\bar{D}^0 \rightarrow K^+\pi^-$ and $B^+ \rightarrow J/\psi(\psi')K^+$ where $J/\psi(\psi') \rightarrow \mu^+\mu^-$ submodes were excluded from the analysis by imposing cuts on the invariant masses of two intermediate particles: $|M(K^+\pi^-) - 1.865| > 0.100 \text{ GeV}/c^2$; $|M(h^+h^-) - 3.097| > 0.070 \text{ GeV}/c^2$; $|M(h^+h^-) - 3.686| > 0.050 \text{ GeV}/c^2$ where h^+ and h^- are pion candidates. The latter two submodes contribute due to the muon-pion misidentification and in these cases we use the muon mass for the $M(h^+h^-)$ calculation.

The M_{bc} and ΔE distributions after excluding these signals are presented in Fig. 1. A significant enhancement in the B signal region can be seen in both distributions.

To determine the intermediate states which contribute to the observed signal, we plot the $K^+\pi^-$ and $\pi^+\pi^-$ invariant mass spectra as shown in Fig. 2. The dashed regions in Fig. 2 show the background spectra determined from M_{bc} and ΔE sidebands. We fit the signal in the $K^+\pi^-$ invariant mass spectrum to the non-coherent sum of two relativistic Breit-Wigner functions. The parameters of the first Breit-Wigner were fixed to be equal to those of the $K^{*o}(892)$ meson and the parameters of the second one referred to as $K_X^{*o}(1400)$ were free during the fit. The signal in the $\pi^+\pi^-$ invariant mass spectrum is fitted to the non-coherent sum of three relativistic Breit-Wigner functions. The parameters of the first and second Breit-Wigners were fixed to be equal to those of $\rho^o(770)$ and $f_o(980)$ mesons respectively and the parameters of the third one referred to as $f_X(1300)$ were free during the fit. Results of the fit are summarized in Table 1.

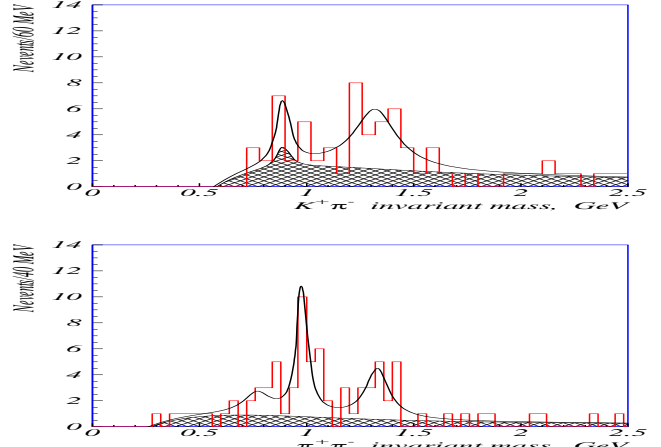


Figure 2: The $K^+\pi^-$ (top) and $\pi^+\pi^-$ (bottom) invariant mass spectra for candidates from the B signal box. Histograms are data and curves are fitting results. The hatched regions are the background estimates from sidebands.

3.2 $B^+ \rightarrow K^+K^+K^-$

We select B candidates formed from three charged tracks identified as kaons. The contribution from the Cabibbo suppressed $B^+ \rightarrow D^0K^+$ decay where $D^0 \rightarrow K^+K^-$, is excluded from the analysis by imposing cuts on the K^+K^- invariant mass: $|M(K^+K^-) - 1.865| > 0.025 \text{ GeV}/c^2$. To suppress the background from $\pi-K$ misidentification we reject all candidates if the invariant mass of any two oppositely charged tracks is consistent within 2σ with the $D \rightarrow K\pi$ hypothesis with the kaon hypothesis assigned to be either of the two tracks. No particle identification information is used in this veto.

The resulting M_{bc} and ΔE distributions are presented in Fig. 3. A large enhancement in the B signal region can be seen in both distributions.

To determine the intermediate states which contribute to the observed signal, we examine the K^+K^- invariant mass spectrum which is shown in Fig. 4. The dashed region in Fig. 4 shows the background spectrum determined from M_{bc} and ΔE sidebands.

The K^+K^- invariant mass spectrum is characterized by two distinct structures. The first one around $1.0 \text{ GeV}/c^2$ is very narrow and corresponds to the $\phi(1020)$ meson. The other one around $1.5 \text{ GeV}/c^2$ which we refer to as $f_X(1500)$ is very broad. We fit the signal in the K^+K^- invariant mass spectrum to the relativistic Breit-Wigner function. The K^+K^- invariant mass region corresponding to the $\phi(1020)$ meson was excluded from the fit. The results of the fit are summarized in Table 1.

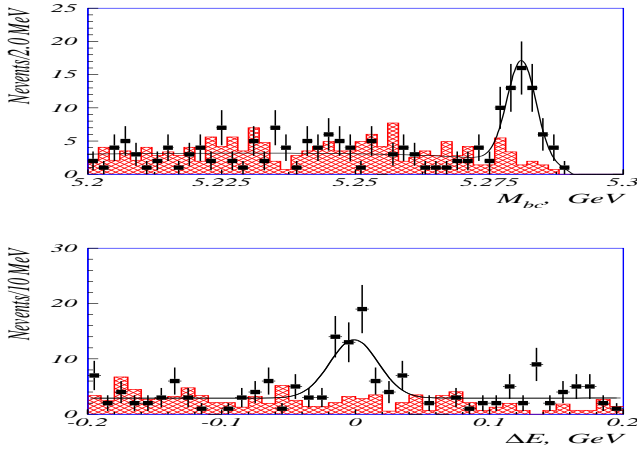


Figure 3: The M_{bc} (top) and ΔE (bottom) distributions for selected $B^+ \rightarrow K^+K^+K^-$ candidates. Points are data and histograms are Monte Carlo expectation for background. Curves are fit to the data.

4 Results

The final signal yield for each submode was extracted from the fit to the beam constrained mass distributions after cuts on the invariant mass of two intermediate particles are applied. We fit the M_{bc} distributions to the sum of a Gaussian function for signal and ARGUS function⁴ for background. We assume that yield in each bin of $K^+\pi^-/\pi^+\pi^-$ is entirely due to a single resonance.

To reduce the systematic error in the branching fractions we normalize our results to the $B^+ \rightarrow \bar{D}^0\pi^+$, $\bar{D}^0 \rightarrow K^+\pi^-$ signal. Similarly, because of poor knowledge of the absolute branching fractions and the uncertainty in the interpretation of some of intermediate resonances, we calculate only the products of the branching fractions rather than their absolute values:

$$\mathcal{B}_{B^+ \rightarrow X h^+} \times \mathcal{B}_{X \rightarrow h^+ h^-} = \frac{N_X}{N_{D\pi}} \times \mathcal{B}_{B \rightarrow D\pi} \times \mathcal{B}_{D \rightarrow K\pi} \times \frac{1}{\delta}$$

where X denotes a h^+h^- resonance state, N_X and $N_{D\pi}$ are the number of observed events for a mode under study and for the reference process respectively, $\mathcal{B}_{B \rightarrow D\pi}$ and $\mathcal{B}_{D \rightarrow K\pi}$ are branching fractions for $B^+ \rightarrow \bar{D}^0\pi^+$ and $\bar{D}^0 \rightarrow K^+\pi^-$ respectively⁵ and δ is the overall correction factor.

5 Discussion & Conclusions

The high quality of π/K separation allowed us to measure for the first time the branching ratios of the three-body decays $B^+ \rightarrow K^+\pi^+\pi^-$ and $B^+ \rightarrow K^+K^+K^-$ without any assumptions about particular intermediate mechanisms. CLEO⁶ and BaBar⁷ have previously

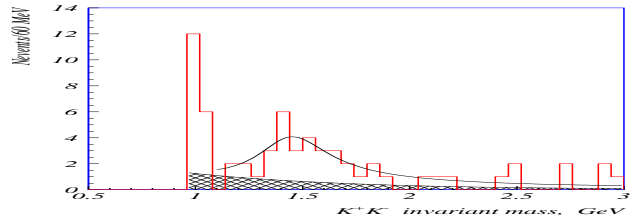


Figure 4: The K^+K^- invariant mass spectrum for candidates from the B signal box. The hatched region is the background estimates from sidebands.

Table 1: Results of the fit to the $K^+\pi^-$, $\pi^+\pi^-$ and K^+K^- invariant mass spectra.

State	M , GeV/c^2	Γ , GeV	Yield
$K^{*o}(892)$	0.896	0.051	8.7 ± 4.7
$K_X^{*o}(1400)$	1.31 ± 0.05	$0.23^{+0.10}_{-0.07}$	28.3 ± 7.4
$\rho^o(770)$	0.769	0.151	10.2 ± 5.8
$f_o(980)$	0.980	0.060	22.8 ± 4.9
$f_X(1300)$	1.33 ± 0.03	$0.13^{+0.07}_{-0.04}$	17.7 ± 6.6
$\phi(1020)$	1019.4	-	14.1 ± 4.6
$f_X(1500)$	1.43 ± 0.08	$0.41^{+0.18}_{-0.18}$	32.8 ± 7.6

placed upper limits on non-resonance three-body decays. The reported numbers for $B^+ \rightarrow K^+\pi^+\pi^-$ (CLEO: $< 28 \times 10^{-6}$, BaBar: $< 66 \times 10^{-6}$) and $B^+ \rightarrow K^+K^+K^-$ (CLEO: $< 38 \times 10^{-6}$) are considerably lower than those presented in this paper. Comparison of the applied selection criteria shows that CLEO and BaBar restricted their analysis to the region of the invariant masses above 2 GeV/c^2 for any pair of the particles. Assuming the phase space distribution of the invariant masses, they obtained the limits quoted above. Similar analysis in our case gives consistent results.

The upper limits obtained for the $K^-\pi^+\pi^+$, $K^+K^-\pi^+$ and $K^+K^+\pi^-$ modes are considerably better than previous results by CLEO⁶ and OPAL⁸. A search for the $K^+K^+\pi^-$ mode is of particular interest since in some extensions of the Standard Model this branching fraction is predicted to be significantly enhanced.

A clear signal has been found in the channel $B^+ \rightarrow K_X^{*o}(1400)\pi^+$, $K_X^{*o}(1400) \rightarrow K^+\pi^-$. Among the resonances in this region, $K_1(1270)$, $K_1(1400)$, $K^*(1410)$, $K_o^*(1430)$ and $K_2^*(1430)$, the first two do not decay into $K\pi$ at all. The branching fraction of $K^*(1410) \rightarrow K\pi$ is too small to make its contribution essential. Thus, only two candidates remain: $K_o^*(1430)$ and $K_2^*(1430)$. However, in the factorization approximation which seems ad-

Table 2: Summary of the results on the search for $B^+ \rightarrow K^+ h^+ h^-$ decays.

Mode	δ	Yield	Sig., σ	$\mathcal{B}(10^{-6})$
$K^+ \pi^+ \pi^-$	0.94	83.0 ± 12.5	8.6	$64.8 \pm 10. \pm 7.0$
$K^+ K^+ K^-$	0.72	48.0 ± 8.0	9.3	$36.5 \pm 6.1 \pm 5.5$
$K^- \pi^+ \pi^+$	0.94	$7.8_{-5.5}^{+6.2}$	—	< 12.8
$K^+ K^- \pi^+$	0.83	$9.7_{-5.9}^{+6.6}$	—	< 17.0
$K^+ K^+ \pi^-$	0.83	$0.0_{-0.0}^{+2.6}$	—	< 5.2

equate in this case, the local production of the tensor $K_2^*(1430)$ is strictly zero⁹. Therefore, its production is only possible due to corrections to the factorizable contribution and most probably is highly suppressed.

In contrast, the scalar meson $K_o^*(1430)$ can be easily produced via the main factorizable contribution and according to a recent estimate¹⁰ the branching fraction for $B^+ \rightarrow K_o^*(1430)\pi^+$ is even larger than that for $B^+ \rightarrow K^o\pi^+$. The prediction gives $\mathcal{B}(B^+ \rightarrow K_o^*(1430)\pi^+) \times \mathcal{B}(K_o^*(1430) \rightarrow K^+\pi^-) \simeq 28 \times 10^{-6}$ which is in good agreement with our result $(23.8_{-5.1}^{+5.6} \pm 5.8) \times 10^{-6}$.

A significant signal was observed for the first time in the decay mode $B^+ \rightarrow f_o(980)K^+$ with a product of branching fraction of $\mathcal{B}(B^+ \rightarrow f_o(980)K^+) \times \mathcal{B}(f_o(980) \rightarrow \pi^+\pi^-) = (16.4_{-4.2}^{+4.9} \pm 2.8) \times 10^{-6}$ also indicates strong coupling of penguins with scalars.

It is not easy to identify a broad state with a mass around 1500 MeV observed in the decay mode $B^+ \rightarrow K^+ K^+ K^-$. If an attempt is made to describe the observed spectrum by a single resonance in addition to the $\phi(1020)$, then it is natural to assume that it is a scalar $s\bar{s}$ state. Such a state is hardly compatible with either one of the scalars $f_o(1370)$ and $f_o(1500)$ suggested by Particle Data Group⁵ and having small probabilities of the decay into $K\bar{K}$ final state. Existence of a state with required properties is predicted in some potential models¹¹ and evidence for such a state was reported by the LASS experiment¹².

Similar uncertainties arise in the interpretation of the peak with a $\pi^+\pi^-$ mass about 1300 MeV in the $K\pi\pi$ system. Two candidates for such a state - $f_2(1270)$ and $f_o(1370)$ exist. The assumption of the $f_o(1370)$ mechanism with its rather small coupling¹³ to $\pi^+\pi^-$ would lead to an unnaturally large branching ratio of the B decay. The parameters of the bump obtained from the fit are close to those of the $f_2(1270)$. However, as recently shown¹⁴, factorization leads to a very small branching ratio for $B^+ \rightarrow f_2(1270)K^+$. If our observation is shown

Table 3: Summary of the results on the search for intermediate resonances in $B^+ \rightarrow K^+\pi^+\pi^-$ and $B^+ \rightarrow K^+K^+K^-$ states.

Mode	δ	Yield	Sig., σ	$\mathcal{B}_{Xh} \times \mathcal{B}_{hh}$ (10^{-6})
$K^{*o}(892)\pi^+$	0.92	$7.5_{-3.4}^{+4.1}$	2.8	< 11.6
$K_X^{*o}(1400)\pi^+$	0.89	$29.1_{-6.3}^{+6.9}$	5.2	$23.8_{-5.1}^{+5.6} \pm 5.8$
$\rho^o(770)K^+$	0.67	$5.5_{-3.4}^{+4.1}$	1.6	< 13.5
$f_o(980)K^+$	0.79	$17.9_{-4.6}^{+5.3}$	4.9	$16.4_{-4.2}^{+4.9} \pm 2.8$
$f_X(1300)K^+$	0.79	$20.4_{-5.0}^{+5.7}$	4.8	$18.8_{-4.6}^{+5.3} \pm 4.3$
$f_X(1500)K^+$	0.45	$20.8_{-4.8}^{+5.5}$	5.5	$25.1_{-5.8}^{+6.6} \pm 4.3$

to be caused by the $f_2(1270)$, then it provides evidence for the nonfactorized contributions which could also account for the large yield of $\eta'K$ in B decays.

Any unambiguous conclusion about the substructure of the observed signal will require a larger data sample which will then allow us to perform the angular analysis of the decay products of the intermediate resonances.

References

1. K. Abe *et al.* (Belle Collaboration), KEK Progress Report 2000-4 (2000), to be published in *Nucl. Instrum. Methods A*.
2. F. Funakoshi *et al.*, Proc. of the 2000 European Particle Accelerator Conference, Vienna (2000).
3. R.A. Fisher, *Ann. Eugenics* **7**, 179 (1936).
4. H. Albrecht *et al.* (ARGUS Collaboration), *Phys. Lett.* **B229**, 304 (1989).
5. D.E. Groom *et al.* (Review of Particle Physics), *Eur. Phys. J.* **C15**, 1 (2000).
6. T. Bergfeld *et al.* (CLEO Collaboration), *Phys. Rev. Lett.* **77**, 4503 (1996).
7. T.J. Champion (BaBar Collaboration), Proc. of the XXXth Int. Conf. on High Energy Phys., Osaka (2000).
8. G. Abbiendi *et al.* (OPAL Collaboration), *Phys. Lett.* **B476**, 233 (2000).
9. G. Buchalla, A.J. Buras and M.E. Lautenbacher, *Rev. Mod. Phys.* **68**, 1125 (1996).
10. V.L. Chernyak, hep-ph/0102217, 2001.
11. E. Klempert, hep-ex/0101031, 2001.
12. D. Aston *et al.* (LASS Collaboration), *Nucl. Phys.* **B301**, 525 (1988).
13. V.V. Anisovich *et al.*, hep-ph/0102338, 2001.
14. C.S. Kim *et al.*, hep-ph/0101292, 2001.